



HAL
open science

Numerical resolution of a physical model of flute-like instruments: comparison between different approaches

Soizic Terrien, Roman Auvray, Benoît Fabre, Pierre-Yves Lagrée, Christophe Vergez

► To cite this version:

Soizic Terrien, Roman Auvray, Benoît Fabre, Pierre-Yves Lagrée, Christophe Vergez. Numerical resolution of a physical model of flute-like instruments: comparison between different approaches. Acoustics 2012, Apr 2012, Nantes, France. hal-00811041

HAL Id: hal-00811041

<https://hal.science/hal-00811041>

Submitted on 23 Apr 2012

HAL is a multi-disciplinary open access archive for the deposit and dissemination of scientific research documents, whether they are published or not. The documents may come from teaching and research institutions in France or abroad, or from public or private research centers.

L'archive ouverte pluridisciplinaire **HAL**, est destinée au dépôt et à la diffusion de documents scientifiques de niveau recherche, publiés ou non, émanant des établissements d'enseignement et de recherche français ou étrangers, des laboratoires publics ou privés.



ACOUSTICS 2012

Numerical resolution of a physical model of flute-like instruments: comparison between different approaches

S. Terrien^a, R. Auvray^b, B. Fabre^b, P.-Y. Lagrée^c and C. Vergez^a

^aLMA - CNRS (UPR 7051), 31 chemin Joseph-Aiguier, 13402 Marseille, Cedex 20, France

^bÉquipe LAM - d'Alembert, 11 rue de Lourmel, 75015 Paris, France

^cCNRS / équipe FCIH - d'Alembert, 4 place Jussieu, 75005 Paris, France
terrien@lma.cnrs-mrs.fr

The study of flute-like instruments involves several subfields of investigation such as acoustics of the waves in the pipe, hydrodynamics of a jet perturbed by an acoustic field and aeroacoustics of a jet/labium interaction. Historically, several models of flute-like instruments have been proposed, including the results from separated studies of the parts mentioned above. In this paper, such a model is written, taking into account the following elements:

- hydrodynamics of a jet perturbed by an acoustic field, through a delay equation, corresponding to the convection of a perturbation of the jet from the flue exit to the labium
- aeroacoustics of a jet/labium interaction, through a nonlinear equation, which highlights the presence of a dipolar pressure source
- acoustics of the waves in the pipe, through a modal formulation
- nonlinear losses at the labium, through an additional nonlinear term

This description includes two nonlinear terms, which require numerical solving. This paper aims at comparing different approaches in terms of the resolution of the nonlinear equations. The following aspects of the model behaviour are addressed: amplitude/frequency evolution along periodic branches, oscillation threshold.

1 Introduction

Since the works of Helmholtz [1], flute-like instruments have been widely studied, and different models have been proposed [2]. They generally include the following elements: hydrodynamics of an unstable jet, aeroacoustic source produced by a jet-labium interaction, acoustic response of a pipe, and a nonlinear term of losses [3]. Even if such a separation between the different terms could be discussed, its validity has been proved [2], and many studies dealing with these elements have been conducted (for example [4, 5, 6] for the jet, [7] for aeroacoustic sources, [8, 9] for the pipe).

However, due to the complex nature of such a model, its global solving is a sensitive issue, and requires numerical tools. Different methods have been proposed (for example [10, 11, 12]), with sometimes important limitations. Since it can be related to the musician/instrument interaction, the study of the solutions evolution with the value of a parameter slowly varying with time is specially interesting, but requires to take into account additional precautions (sections 2 and 4). We propose to compare different numerical solving methods, focusing on oscillation threshold, and oscillating amplitude/frequency evolutions along the periodic solution branches.

In the first section, we briefly recall the mechanism of sound production in flute-like instruments and we describe the simplified model. Then, we present the different resolution methods, and in section 4, we compare the results provided by these different approaches.

2 Physical model of flute-like instruments

2.1 Mechanism of sound production

2.1.1 General description

A classical approach in musical acoustics consists in describing an instrument by a nonlinear coupling between an exciter and a resonator [13]. In flute-like instruments, the exciter consists of the interaction between an air jet and an edge called “labium” (see Fig. 1).

More precisely, when the musician blows in the instrument, an unstable jet is generated at the channel exit. The interaction between this jet and the labium constitutes an aeroacoustic source, exciting the resonator. The acoustic field thus created in the pipe, in turn, perturbs the jet at the channel exit. This perturbation is amplified and convected along the jet towards the labium, and so sustains the oscillations of the

jet around the labium. Closing the feedback loop, this mechanism allows the establishment of auto-oscillations.

To correctly model the saturation of the oscillating amplitude, a term of dissipation must be taken into account, which describes the vortex shedding at the labium. In this section, we first briefly describe the behaviour of these different elements, and we secondly present the studied model and the simplifications on which it is based.

In flute-like instruments, the jet velocity U_j is an important parameter. Indeed, it is directly related to the slowly varying pressure in the musician’s mouth, and so associated to the fact that the instrumentalist blows hard or not. As we will see below, it is thus particularly interesting to study the evolution of the model solutions with the value of this parameter.

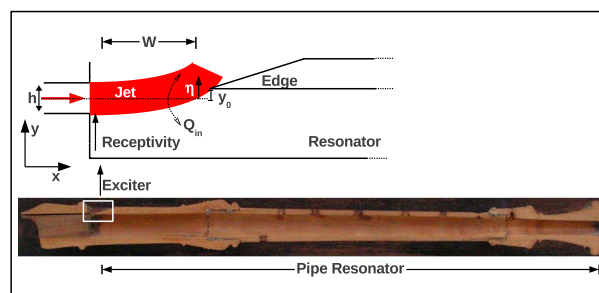


Figure 1: Simplified representation of the excitation window of a recorder.

2.1.2 Hydrodynamics of the jet

In flute-like instruments, the initial perturbation of the jet is provided by the acoustic field present in the pipe resonator. This phenomenon, called “receptivity”, has been studied by De la Cuadra [5]. Based on experimental works, he proposed the following expression for the initial perturbation of the jet at the channel exit:

$$\eta_0(t) = h \frac{v_{ac}(t)}{U_j}, \quad (1)$$

where η_0 is the transversal displacement of the jet at the channel exit, h the height of the channel exit, v_{ac} the oscillating amplitude of the acoustic velocity at the pipe exit, and U_j the jet central velocity.

Since the works of Rayleigh [14], it is known that the convection of a perturbation along a naturally unstable jet is accompanied by its amplification. As a first approximation, a linear model, such as that proposed by Rayleigh, predicts

an exponential amplification with respect to the distance x : $\eta(x) = \eta_0 \cdot e^{\alpha_i x}$ where α_i is the amplification parameter. De la Cuadra [5] proposed the empirical expression $\alpha_i \approx \frac{0.4}{h}$. The combination of this element with Eq. (1) leads to the transversal perturbation of the jet at the labium:

$$\eta(W, t) = e^{\alpha_i W} \eta_0(t - \tau) = \frac{h}{U_j} e^{\alpha_i W} v_{ac}(t - \tau), \quad (2)$$

where W is the distance between the channel exit and the labium (see Fig. 1), and τ the convection delay of the perturbation along the jet, given by: $\tau = \frac{W}{c_p}$ with c_p the convection velocity of perturbations along the jet. Theoretical [14] and experimental [5] works have shown that $0.3U_j \leq c_p \leq 0.5U_j$. We retain $c_p = 0.4U_j$, and consider the following realistic values for a recorder: $W = 4\text{mm}$ and $h = 1\text{mm}$.

2.1.3 Nonlinear jet-labium interaction: aero-acoustic source

The oscillation of the jet around the labium (see Fig. 1) corresponds to a flow injection alternately inside and outside the pipe. Following the jet-drive model developed by Verge [4], we represent this alternative flow injection as a pressure difference $\Delta p = p_{in} - p_{out}$ between the two sides of the labium (p_{in} is the pressure in the pipe, and p_{out} the external pressure):

$$\Delta p = -\frac{\rho \delta_d}{S_w} \cdot \frac{dQ_{in}}{dt}, \quad (3)$$

where ρ is the air density, δ_d the effective distance between the two flow sources, $S_w = WH$ the surface area of the window between the channel exit and the labium, and H the width of this window. Assuming that each flow source is located at a distance h of the labium, Verge [4] calculated: $\delta_d = \frac{4}{\pi} \sqrt{2hW}$. Q_{in} , the part of the flow injecting in the pipe, is given by:

$$Q_{in} = \langle H \int_{-\infty}^{y_0 - \eta(t)} U(y) dy \rangle, \quad (4)$$

with y_0 the offset between the labium and the channel exit (see Fig. 1), and $U(y)$ the jet velocity. Representing the bell-shape of the jet by a Bickley profile $U(y) = U_j \text{sech}\left(\frac{y}{b}\right)^2$, with b the half width of the jet, leads to the pressure difference:

$$\Delta p(t) = \frac{\rho \delta_d b U_j}{W} \cdot \frac{d}{dt} \left[\tanh\left(\frac{\eta(t) - y_0}{b}\right) \right]. \quad (5)$$

This pressure difference represents the acoustic force exerted by the jet/edge interaction on the air column, and thus constitutes the aeroacoustic source that excites the resonator.

2.1.4 Acoustical response of the pipe

The resonator, constituted by the air column in the pipe, amplifies the acoustic oscillations near its resonance frequencies. As the exciter involves a pressure source, the acoustical response of the pipe can be represented through its input admittance $Y_{in} = \frac{V_{ac}}{\Delta P}$, where V_{ac} and ΔP are respectively the acoustical velocity and the term of pressure source, in the frequency domain (*i.e.* for ΔP the Fourier transform of Eq. (5)). Using a modal decomposition, we write the input admittance in the frequency domain as a sum of m resonance modes:

$$Y_{in} = \sum_m \frac{a_m j \omega}{\omega_m^2 - \omega^2 + j \omega \frac{\omega_m}{Q_m}}, \quad (6)$$

where a_m , ω_m and Q_m are respectively the modal amplitude, the resonance pulsation and the quality factor of the m^{th} resonance mode.

2.1.5 Nonlinear losses at the labium

In most flute-like instruments, the surface area of the window between the channel exit and the labium is smaller than the cross section of the pipe. Therefore, the window represents a constriction for the acoustic flow, which causes the separation of the flow at the labium, and leads to the formation and the shedding of vortices on the jet [3]. One can model this phenomenon as a variation of the pressure difference between the two sides of the labium. It results in an additional nonlinear term in Eq. (5) representing the aeroacoustical source:

$$\Delta p(t) = \frac{\rho \delta_d b U_j}{W} \frac{d}{dt} \left[\tanh\left(\frac{\eta(t) - y_0}{b}\right) \right] - \frac{\rho}{2 \alpha_{vc}^2} \text{sgn}(v_{ac}), \quad (7)$$

where $\alpha_{vc} \approx 0.6$ is the *vena-contracta* factor [3].

2.2 Simplified model

In order to simplify the study, we take into account a single acoustic mode of the resonator (that is to say a single term in Eq. (6)), with $a_1 = 28$, $Q_1 = 40$, and $f_1 = 500$ Hz.

Writing Eq. (6) in the time-domain leads to:

$$\ddot{v}_{ac}(t) + \frac{\omega_1}{Q_1} \dot{v}_{ac}(t) + \omega_1^2 v_{ac}(t) = a_1 \dot{\Delta p}. \quad (8)$$

Assuming that the jet velocity U_j varies slowly compared to the other variables, its derivatives can be neglected. Then injecting Eqs. (7) and (2) in this expression, we obtain:

$$\ddot{v}_{ac}(t) = \frac{a_1 \rho \delta_d b U_j}{W} \frac{d^2}{dt^2} \left\{ \tanh\left[\frac{h e^{\alpha_i W} v_{ac}(t - \tau) - y_0}{b U_j} \right] - \frac{\rho}{2} \left(\frac{v_{ac}}{\alpha_{vc}} \right)^2 \text{sgn}(v_{ac}) \right\} - \frac{\omega_1}{Q_1} \dot{v}_{ac}(t) - \omega_1^2 v_{ac}(t). \quad (9)$$

To simplify numerical issues, it is helpful to make the system dimensionless. We define a dimensionless time $\tilde{t} = \omega_1 t$ and a dimensionless acoustical velocity $\tilde{v}(\tilde{t}) = \frac{h e^{\alpha_i W}}{b U_j} v_{ac}(\tilde{t})$. Injecting these expressions in Eq. (9) finally yields:

$$\ddot{\tilde{v}}(\tilde{t}) = \frac{a_1 \rho \delta_d b U_j}{W} \frac{d^2}{d\tilde{t}^2} \left\{ \tanh\left[\tilde{v}(\tilde{t} - \tilde{\tau}) - \frac{y_0}{b} \right] - \frac{\rho}{2 e^{2\alpha_i W}} \left(\frac{b U_j}{h \alpha_{vc}} \right)^2 \tilde{v}(\tilde{t})^2 \right\} - \frac{\dot{\tilde{v}}(\tilde{t})}{Q_1} - \tilde{v}(\tilde{t}), \quad (10)$$

where $\dot{\tilde{v}}$ is the derivative of variable \tilde{v} with respect to dimensionless time \tilde{t} .

3 Resolution of the model: different approaches

Due to the presence of two nonlinear terms in Eq. (10), analytical resolution is not possible, and the study of the model requires the use of numerical methods.

Moreover, the presence of a delayed term in the derivative part of Eq. (10) highlights the *neutral* nature of the studied model. This feature increases the model complexity [15], and its accurate analysis requires the use of particular numerical methods described in this section.

3.1 Linear Analysis

Although accurate results can only be obtained while solving the nonlinear equations, linearization of the studied system around the trivial solution $\Delta p = \eta = v_{ac} = 0$ allows to

obtain a first approximation of different results. In a feedback loop system such as the one presented in the previous section, it is known that the emergence of auto-oscillations is possible under the necessary (but not sufficient) following conditions on the linearised open-loop gain G [16]:

- $|G|$ must be larger than 1.
- $\arg(G)$ must be a multiple of 2π .

As demonstrated in [12], the linearization of the studied system leads to the open loop gain (in the frequency domain):

$$G = j\omega \frac{h\rho\delta_d e^{\alpha_i W}}{W} Y_{in}(\omega) e^{-j\omega\tau}. \quad (11)$$

The second condition applied to this equation leads to:

$$-\omega_p\tau + \frac{\pi}{2} + \arg[Y_{in}(\omega_p)] = -2n\pi. \quad (12)$$

The solution ω_p of this equation yields a first approximation of the oscillating frequency of the studied model. Although this reasoning is rigorously valid only at the oscillation threshold, previous studies have shown that it provides good approximations along the whole solutions branch [12]. The integer n is related to the order of the hydrodynamic mode of the jet: the case $n = 0$ corresponds to the first hydrodynamic mode, that one can observe on flute-like instruments in normal playing conditions [5]. The higher values of n correspond to ‘‘aeolian modes’’, which are particular sounds obtained at very low jet velocity [3].

3.2 Time-domain simulations

We compare the results provided by several classical time-domain approaches, based on different numerical schemes adapted to neutral delay differential equations:

1. An iterative algorithm based on a fourth-order Runge Kutta method (RK4). The delayed sample is estimated by a linear interpolation of the previous calculated samples. The jet velocity is allowed to vary with a piecewise shape between three target values. The jet velocity must verify a quasi-steady condition because its derivatives have been neglected in Eq. (10) (see [12] for more details). The oscillation is initiated by holding the variable y constant at an arbitrary value for negative time. It results in a short transient, with no physical meaning, after which the system evolves freely.
2. A Bogacki-Shampine scheme with adaptative step-size, implemented in the Simulink/Matlab solver ode23 [17]. As above, the delayed samples are estimated by a linear interpolation between to computed samples.
3. A ‘‘dissipative’’ approach (ddeNsd), especially developed to solve neutral delay differential equations [18]. It consists in approximating the neutral equation:

$$y'(t) = f[t, y(t), y(t - \tau), y'(t - \tau)] \quad (13)$$

by the delay differential equation:

$$z'(t) = f\left(t, z(t), z(t - \tau), \frac{z(t - \tau) - z(t - \tau - \delta)}{\delta}\right) \quad (14)$$

and in resolving this system with a Matlab solver (namely ddesd), developed for delay differential equations [19]. This solver, which originally does not support neutral systems, is based on an explicit Runge Kutta scheme with continuous extension to evaluate the delayed variables.

3.3 Numerical continuation

The use of numerical continuation has recently shown to be useful in the context of musical acoustics [20]. Indeed, it permits to calculate bifurcation diagrams, which represent, ideally, all the periodic solutions of the studied model, as a function of one of the system parameters (called the ‘‘continuation parameter’’). It thus provides a more global knowledge of the system dynamics: existence of unstable solutions, coexistence of several solutions (which explains, for example, hysteresis phenomena)...

The neutral nature of the model prevents us from using classical softwares as AUTO [21] or MANLAB [22]: we use here NDDE-Biftool [15, 23], especially adapted for numerical continuation of neutral delay differential equations. Periodic solutions are computed using orthogonal collocation: a single period T of the solution $x(t)$ is discretized, leading to a set of discrete points $\{x(t_0), x(t_1), \dots, x(t_N = t_0 + T) = x(t_0)\}$ which are, together with the period T , the unknowns (see for example [24] for more details).

Knowing a solution x_0 for a set of parameters λ_0 , one can compute the whole corresponding branch of periodic solutions passing through $x = x_0$ at $\lambda = \lambda_0$. In NDDE-Biftool, numerical continuation relies on a classical Prediction-Correction Method: starting from the given solution x_0 , an approximation of a neighboring solution (corresponding to a set of parameters $\lambda_0 + \Delta\lambda$) is computed using a tangent predictor. To avoid difficulties on the return points where the tangent tends to infinity, the branch is parameterized using the Keller’s pseudo arc-length (see for example [25]). This first approximation is then corrected using an iterative correction algorithm based on Newton method. Step by step, this approach allows to compute the whole periodic solution branch.

4 Results and discussions: comparison between the different approaches

In a musical context, it is particularly interesting to compare the results provided by the different resolution methods in terms of oscillating amplitude, oscillating frequency, and oscillation threshold. Indeed, these variables are directly related to the sound intensity (for the amplitude), and to the pitch of the note (for the frequency). Since we only take into account a single resonance mode of the pipe, we do not address here the sound spectrum.

For each numerical method, the user can adjust some parameters affecting both accuracy and convergence of the results:

- the sampling frequency, the relative tolerance, and the rate of change of parameter U_j for time-domain solver ode23. For the time-domain solvers RK4 and ddeNsd, the user controls, in addition, the initial condition defined above.
- the number of points per period, the relative tolerance, the maximal step of the bifurcation parameter between two successive points of the branch, and the use of an adaptative mesh for numerical continuation.

Thus, computing numerical solutions always relies on a compromise between results accuracy and computation time.

As it is classical for flute-like instruments, we define, to represent the results, the dimensionless jet velocity $\theta = \frac{U_j}{W f_j}$ [12].

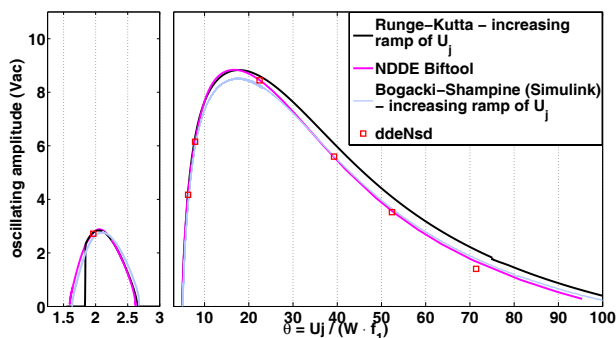


Figure 2: Oscillating amplitude of v_{ac} (m/s) versus dimensionless jet velocity θ for the different solving methods. Left: aeolian regime. Right: “standard” regime.

4.1 Oscillating amplitude

Fig. 2 represents the oscillating amplitude of the variable v_{ac} as a function of the dimensionless jet velocity θ . Globally, this representation shows good agreement between the different numerical solving methods, for both aeolian and standard regimes. However, as shown on Fig. 3, the relative difference between the results provided by time-domain solvers and those provided by numerical continuation highlights significant differences on several parts of the branches. Moreover, we observe that for a given time-domain solver (for example those based on a fourth-order Runge-Kutta scheme), the difference is small (lower than 5%) at the top of the branch, whereas it reaches 25% around $\theta = 70$. It would probably be possible to reduce these differences by further adapting the different numerical parameters mentioned above. However, obtaining the plotted results with time-domain simulations already requires a high sampling frequency (up to 1MHz and 160kHz respectively for the Bogacki-Shampine and the fourth-order Runge Kutta solvers), and a slow variation in time of the jet velocity U_j , in order to comply with the quasi-static hypothesis (section 2). Consequently, some of these calculations are CPU demanding (a few hours for the Bogacki-Shampine solver). The fourth-order Runge-Kutta scheme is more efficient (about 5 minutes for the plotted data), but this time calculation is very sensitive to the numerical parameter values. Moreover, it is sometimes necessary to repeat several times the same calculation in order to choose convenient numerical parameters. Computing more accurate results with these time-domain solvers is thus hardly conceivable for an user aiming at studying the influence of the model parameters. On the other hand, if the implementation of a given model in the numerical continuation software can first present important numerical issues, the study of the influence of the parameter modifications is then, most of the time, more easy and not so CPU-demanding (about 15 minutes for the two plotted periodic solution branches).

4.2 Oscillation threshold

As shown on Fig. 3, oscillation thresholds are particularly sensitive zones. For sake of clarity, Figs. 2 and 3 represent only the results of time-domain simulations for increasing ramps of the jet velocity U_j . Indeed, differences between increasing and decreasing ramps are not visible at this scale. Fig. 4 focus on the oscillation threshold of the standard regime, and shows, for one of the time-domain solver (fourth-order Runge-Kutta scheme), an hysteresis effect on the threshold, between an increasing and a decreasing ramp of the jet velocity U_j . An hysteresis phenomenon is related to the coexistence of two stable solutions of the model for the

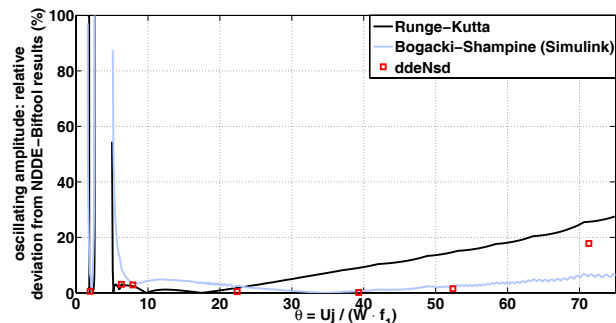


Figure 3: Relative difference between the oscillating amplitude computed by NDDE-Biftool (numerical continuation) and those provided by time-domain solvers.

same parameter values. The bifurcation diagram provided by NDDE-Biftool shows only one stable solution, highlighting that this hysteresis effect is purely numerical: varying the bifurcation parameter U_j with respect to time, even very slowly, is not completely consistent with the quasi-static hypothesis.

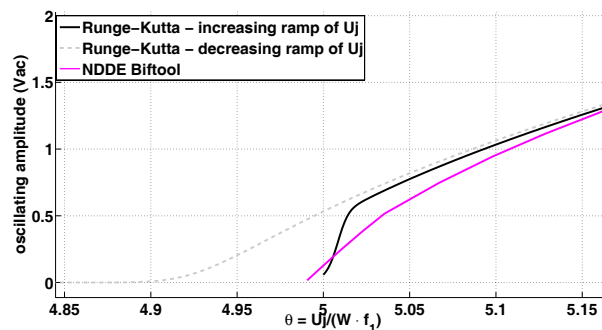


Figure 4: Oscillating amplitude of variable v_{ac} (m/s) versus dimensionless jet velocity θ : zoom around the oscillation threshold of the “standard” regime.

4.3 Oscillating frequency

Fig. 5 represents the oscillating frequency versus the dimensionless jet velocity θ . For the different numerical solving methods of the nonlinear model, we observe a common global shape of frequency evolution along the branches. However, differences up to 2% to 3% occur between one of the time-domain solver (Bogacki-Shampine scheme) and the others numerical methods. If such a deviation may seem small, it is significant for a frequency value: indeed, it corresponds to about 50 cents, thus, in a musical context, to a quarter tone. Contrary to what is observed for the amplitude, this frequency offset does not seem altered by the change of the sampling frequency or the rate of change of the jet velocity U_j , and it thus seems intrinsic to the numerical scheme. Furthermore, one can observe that numerical methods especially dedicated to the analysis of neutral delay differential equations (namely the “dissipative” solver ddeNsd, the Runge-Kutta solver, and NDDE-Biftool) seem to provide concordant results. Conversely, the more general solver based on a Bogacki-Shampine scheme (implemented in Simulink) provides frequency values further away from the others. Moreover, Fig. 5 shows that if the linear analysis leads to a first approximation of the order of magnitude of the oscillating frequency, it provides neither an accurate value outside the vicinity of the oscillation threshold, nor a good approxi-

mation of the frequency evolution shape along the branch.

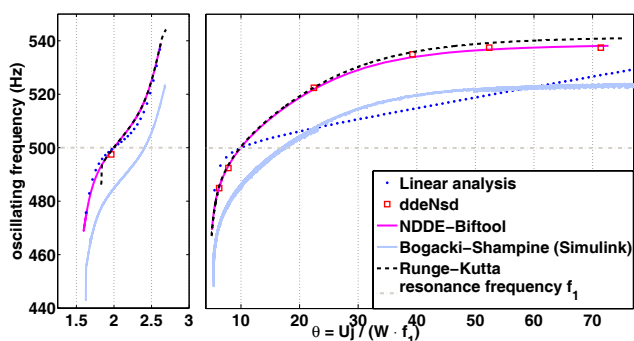


Figure 5: Oscillating frequency (Hz) versus dimensionless jet velocity θ for the different solving methods. Left: aeolian regime. Right: "standard" regime.

5 Conclusion

For very low computational cost, the linear analysis provides useful informations, for instance on the oscillating frequency. However, solving the whole nonlinear system is necessary to calculate accurate solutions. Results obtained by the different numerical approaches are globally consistent, but this comparison highlights the importance of using tools especially developed for the study of neutral delay differential equations. Indeed, results provided by this kind of methods seem to be more accurate than those obtained using more general numerical schemes.

Nevertheless, such resolutions are still demanding in computation time, and the choice of numerical parameters as, for example, the sampling frequency for the time-domain solvers or the number of points per period for numerical continuation is very important to obtain accurate results.

Finally, it is important to keep in mind that this simplified model takes into account a single acoustic mode of the pipe. We can assume that several characteristics, as for example the frequency evolution along the branches or the solutions stability would be affected by the addition of other acoustic modes.

References

- [1] H. von Helmholtz, *On the Sensation of Tones*, Dover ed., New York (1954)
- [2] B. Fabre, A. Hirschberg, "Physical Modeling of Flue Instruments: A Review of Lumped Models", *Acta Acustica united with Acustica* **86**, 599-610 (2000)
- [3] A. Chaigne, J. Kergomard, *Acoustique des instruments de musique*, Belin ed., Paris (2008)
- [4] M.P. Verge, R. Causse, B. Fabre, A. Hirschberg, A.P.J. Widjnands, A. van Steenberg, "Jet oscillations and jet drive in recorder-like instruments", *Acta Acustica united with Acustica* **2**, 403-419 (1994)
- [5] P. de la Cuadra, C. Vergez, B. Fabre, "Visualization and analysis of jet oscillation under transverse acoustic perturbation", *Journal of Flow Visualization and Image Processing* **14**(4), 355-374 (2007)
- [6] N.H. Fletcher, "Jet drive mechanism in organ pipes", *J. Acoust. Soc. Am.* **60**, 481-483 (1976)
- [7] M. Meissner, "Aerodynamically excited acoustic oscillations in cavity resonator exposed to an air jet", *Acta Acustica united with Acustica* **88**, 170-180 (2001)
- [8] D.H. Lyons, "Resonance frequencies of the recorder (english flute)", *J. Acoust. Soc. Am.* **70**, 1239-1247 (1981)
- [9] J.W. Coltman, "Resonance and sounding frequencies of the flute", *J. Acoust. Soc. Am.* **40**, 99-107 (1966)
- [10] N.H. Fletcher, "Sound production by organ flue pipes", *J. Acoust. Soc. Am.* **60**(4), 926-936 (1976)
- [11] R.T. Schumacher, "Self-sustained oscillations of organ flue pipes: an integral equation solution", *Acustica* **39**, 225-238 (1978)
- [12] R. Auvray, B. Fabre, P.-Y. Lagrée, "Regime change and oscillation thresholds in recorder-like instruments", *J. Acoust. Soc. Am.* **131**(2), 1574-1585 (2012)
- [13] M.E. McIntyre, R.T. Schumacher, J. Woodhouse, "On the oscillations of musical instruments", *J. Acous. Soc. Am.* **74**(5), 1325-1345 (1983)
- [14] J.W.S. Rayleigh, *The theory of sound*, Dover ed., New York (1877)
- [15] D. Barton, B. Krauskopf, R.E. Wilson, "Collocation schemes for periodic solutions of neutral delay differential equations", *Journal of Difference Equations and Applications* **12**(11), 1087-1101 (2006)
- [16] N.H. Fletcher, "Autonomous vibration of simple pressure-controlled valves in gas flows", *J. Acous. Soc. Am.* **93**(4), 2172-2180 (1993)
- [17] P. Bogacki, L.F. Shampine, "A 3(2) pair of Runge-Kutta formulas", *Applied Mathematics Letter* **2**(4), 231-325 (1989)
- [18] L.F. Shampine, "Dissipative Approximations to Neutral DDEs", *Applied Mathematics and Computation* **203**(2), 641-648 (2008)
- [19] L.F. Shampine, "Solving ODEs and DDEs with residual control", *Applied Numerical Mathematics* **52**(1), 113-127 (2005)
- [20] S. Karkar, C. Vergez, B. Cochelin, "Oscillation threshold of a clarinet model: a numerical continuation approach", *J. Acoust. Soc. Am.* **131**(1), 698-707 (2012)
- [21] E.J. Doedel, "AUTO: A Program For Automatic Bifurcation Analysis of Autonomous Systems", *Congressus Numerantium* **30**, 265-284 (1981)
- [22] B. Cochelin, C. Vergez, "A high order purely frequency-based harmonic balance formulation for continuation of periodic solutions", *Journal of Sound and Vibration* **324**, 243-262 (2009)
- [23] K. Engelborghs, "DDE-Biftool: a Matlab package for bifurcation analysis of delay differential equations", Katholieke Universiteit Leuven, (2000)
- [24] K. Engelborghs, T. Luzyanina, K.J. in't Hout, D. Roose, "Collocation Methods for the Computation of Periodic Solutions of Delay Differential Equations", *SIAM Journal on Scientific Computing* **22**(5), 1593-1609 (2000)
- [25] B. Cochelin, N. Damil, M. Potier-Ferry, *Méthode asymptotique numérique*, Lavoisier ed., Paris (2007)